Structural Engineering and Mechanics, *Vol. 70, No. 4 (2019) 407-420*
DOI: https://doi.org/10.12989/sem.2019.70.4.407

Influence of shear preload on wave propagation in small-scale plates with nanofibers

M.R. Farajpour[1], A.R. Shahidi*[2] and A. Farajpour[2]

[1]Borjavaran Center of Applied Science and Technology, University of Applied Sciences and Technology, Tehran, Iran
[2]Department of Mechanical Engineering, Isfahan University of Technology, Isfahan 8415683111, Iran

(Received December 22, 2018, Revised February 26, 2019, Accepted March 17, 2019)

Abstract. In the present work, an attempt is made to explore the effects of shear in-plane preload on the wave propagation response of small-scale plates containing nanofibers. The small-scale system is assumed to be embedded in an elastic matrix. The nonlocal elasticity is utilized in order to develop a size-dependent model of plates. The proposed plate model is able to describe both nanofiber effects and the influences of being at small-scales on the wave propagation response. The size-dependent differential equations are derived for motions along all directions. The size-dependent coupled equations are solved analytically to obtain the phase and group velocities of the small-scale plate under a shear in-plane preload. The effects of this shear preload in conjunction with nanofiber and size effects as well as the influences of the elastic matrix on the wave propagation response are analyzed in detail.

Keywords: shear preload; nanofibers; small-scale plates; size effects

1. Introduction

Small-scale plates and beams such as microscale and nanoscale sheets and tubes operate as the fundamental parts of many ultrasmall devices since they display excellent electromechanical properties. In many applications, there are electromechanical loads exerted on small-scale plates and beams, which are originated from different sources such as electromagnetic fields and initial stresses. To better design the manufacturing process, it is important to understand the mechanical response of small-scale plates and beams under different loading conditions.

The mechanical response of nanostructures including nanoplates (Asemi *et al*. 2014, Bakhadda *et al*. 2018, Bouadi *et al*. 2018, Kadari *et al*. 2018, Mokhtar *et al*. 2018, Yazid *et al*. 2018), nanobeams (Chaht *et al*. 2015, Zemri *et al*. 2015, Ahouel *et al*. 2016, Bellifa *et al*. 2017, Nejad *et al*. 2017, Farajpour *et al*. 2018, Hamza-Cherif *et al*. 2018) and nanoshells (Farajpour and Rastgoo 2017, Karami *et al*. 2018) has been analyzed in the literature using a number of size-dependent continuum models such as nonlocal four variable model (Belkorissat *et al*. 2015), trigonometric theory of shear deformations (Besseghier *et al*. 2017, Khetir *et al*. 2017, Mouffoki *et al*. 2017), nonlocal zeroth-order theory of shear deformations (Bounouara *et al*. 2016), nonlocal quasi-3D theory (Bouafia *et al*. 2017), surface elasticity (Youcef, Kaci *et al*. 2018) and nonlocal strain gradient theory (Farajpour and Rastgoo 2017, Farajpour *et al*. 2018). On the other hand, in addition to the wave propagation analysis of macroscale structures (Yahia *et al*. 2015, Fourn *et al*. 2018), wave propagation characteristics of small-scale structures (Karami *et al*. 2018) using size-dependent theories (Karami *et al*. 2017, Karami *et al*. 2018) have been analyzed.

The influences of mechanical preload caused by initial stresses on the mechanical behaviors of small-scale beams were analyzed in the last decade using continuum-based models. Classical scale-free continuum mechanics cannot be utilized for nanobeams under mechanical preload since it does not capture size effects (Chakraverty and Behera 2015, Kiani *et al*. 2017, Ebrahimi and Barati 2018, Ebrahimi and Barati 2018, Ebrahimi and Barati 2018, Ebrahimi and Heidari 2018, Ma *et al*. 2018). A few size-dependent continuum-based models have been proposed for analyzing the stability, vibration and bending of small-scale structures (Malekzadeh and Shojaee 2013, Farajpour *et al*. 2014, Shenas and Malekzadeh 2016, Farajpour *et al*. 2017, Ebrahimi and Barati 2018). Wang and Cai (Wang and Cai 2006) explored the effects of mechanical preload on the vibrations of a system of nanoscale tubes with the help of a continuum-based theory. In another study conducted by Song *et al*. (Song *et al*. 2010), the influences of axial preload on the wave propagations in nanoscale tubes were scrutinized employing the nonlocal theory. In addition, sound wave propagation characteristics of a single nanotube were extracted by Heireche *et al*. (Heireche *et al*. 2008) using a nonlocal model together with an analytical solution approach. The influences of axial preload as well as the effects of a magnetic field on the vibration of nanotubes were also studied in Ref. (Güven 2014). Moreover, the effects of compressive preload on the wave propagation in nanoscale tubes were investigated with the help of a continuum model (Selim *et al*. 2009). A nonlocal beam model was also proposed in the literature for analyzing the effects of axial preload on the frequency shifts of a

*Corresponding author, Assistant Professor
E-mail: shahidi@cc.iut.ac.ir

http://www.techno-press.com/journals/sem&subpage=7
ISSN: 1225-4568 (Print), 1598-6217 (Online)

nanomechanical sensor using two vibrating nanotubes (Shen *et al*. 2012).

In addition to the application of size-dependent models in analyzing small-scale tubes under axial preload, the mechanical behaviors of small-scale plates subjected to in-plane preload have been examined. A size-dependent model was introduced by Asemi *et al*. (Asemi *et al*. 2014) to investigate the effects of in-plane preload caused by initial stresses on the vibrations of nanoscale plates made of piezoelectric materials with the help of the nonlocal theory. Furthermore, the wave propagation features of small-scale plates subjected to in-plane preload were obtained in Ref. (Wang *et al*. 2010) employing the nonlocal theory. In another study reported in Ref. (Murmu and Pradhan 2009), the transverse vibration of nanoscale plates under uniaxial preload was investigated applying the nonlocal theory. The effects of an elastic substrate in conjunction with the influences of in-plane preload on the wave propagation in graphene sheets were scrutinized by Karami *et al*. (Karami *et al*. 2018). Mohammadi *et al*. (Mohammadi *et al*. 2014) examined the influences of an elastic medium and the effects of shear in-plane preload on the natural frequencies of small-scale plates. In another study, Ebrahimi and Shafiei (Ebrahimi and Shafiei 2017) used a combination of the nonlocal theory and Reddy's shear deformation model of plates to analyze the vibrations of small-scale plates subjected to in-plane preload.

In all of the above-stated valuable works, only the influence of initial load on the mechanics of a simple homogeneous small-scale structure without any kind of reinforcement is investigated. With the development of advanced manufacturing techniques at small-scales, more complex micro/nanoscale structures with superior electromechanical properties have successfully been synthesized. For instance, shape memory alloy (SMA) properties have lately been observed in a couple of small-scale fundamental structures such as nanofibers and nanofilms (Kahn *et al*. 1998). From the literature review, it can be seen that no size-dependent continuum model has been developed for investigating the influences of shear in-plane preload on the elastic wave dispersion in small-scale plates containing nanofibers. To ensure consistency between the continuum model and real operating conditions, it is assumed that the plate is embedded in an elastic matrix. The nonlocal elasticity, as a modified scale-dependent theory, is used to model the problem. The size-dependent motion equations are then derived along all directions. The phase and group velocities of the small-scale system subjected to shear in-plane preload are analytically obtained. The influences of shear preload and elastic matrix as well as size and nanofiber effects on the elastic wave dispersion in the nanosystem containing nanofibers are explored.

2. Small-scale plates containing nanofibers

In the following, the elastic wave dispersion in small-scale plates containing nanofibers is modeled based on a combination of Brinson's model and nonlocal theory. Figure 1 indicates a system of five small-scale plates and nanofibers. It is assumed that a uniform shear in-plane preload is exerted on the system as shown in the figure. In addition, the system is embedded in an elastic matrix with shear stiffness coefficient k_s and normal stiffness coefficient k_n (Akgöz and Civalek 2013, Civalek 2013).

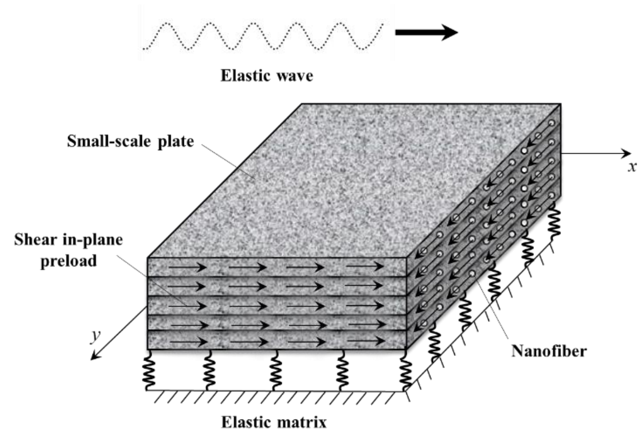

Fig. 1 Elastic waves in small-scale plates under shear preload containing nanofibers

For the geometrical properties of each layer, we assume that (length, thickness, width) = (a, h, b). Furthermore, for the elastic and physical properties, one can write (shear modulus, elasticity modulus, density, Poisson's ratio) = (G_{12}^{sys}, E_i^{sys}, ρ_{sys}, v_{12}^{sys}) in which "sys" is an abbreviation for "system". These elastic and physical properties are written as (Park *et al*. 2004)

$$\begin{aligned}
&E_1^{sys}(\zeta)=\left(V_F(\zeta)\right)E_F+\left(1-V_F(\zeta)\right)E_L,\\
&\rho_{sys}(\zeta)=\left(V_F(\zeta)\right)\rho_F+\left(1-V_F(\zeta)\right)\rho_L,\\
&v_{12}^{sys}(\zeta)=\left(V_F(\zeta)\right)v_F+\left(1-V_F(\zeta)\right)v_L,\\
&E_2^{sys}(\zeta)=\frac{E_F E_L}{\left(V_F(\zeta)\right)E_L+\left(1-V_F(\zeta)\right)E_F},\\
&G_{12}^{sys}(\zeta)=\frac{G_F G_L}{\left(V_F(\zeta)\right)G_L+\left(1-V_F(\zeta)\right)G_F},
\end{aligned} \tag{1}$$

in which "F" is employed to represent nanoscale fibers whereas "L" denotes each layer without nanofibers, V_F and ζ represent the volume fraction of fibers and martensite fraction, respectively. In Appendix A, the basic equations for SMA nanofibers, as a particular type of nanofibers, are given. The in-plane strains of the small-scale system are as (Reddy 2010, Aksencer and Aydogdu 2011)

$$\begin{aligned}
\varepsilon_{xx}&=e_{xx}^0-z\kappa_{xx},\\
\varepsilon_{yy}&=e_{yy}^0-z\kappa_{yy},\\
\gamma_{xy}&=\gamma_{xy}^0-z\kappa_{xy},
\end{aligned} \tag{2}$$

where

$$\begin{aligned}
&e_{xx}^0=\frac{\partial u}{\partial x},\quad e_{yy}^0=\frac{\partial v}{\partial y},\quad \gamma_{xy}^0=\frac{\partial v}{\partial x}+\frac{\partial u}{\partial y},\\
&\kappa_{xx}=\frac{\partial^2 w}{\partial x^2},\quad \kappa_{yy}=\frac{\partial^2 w}{\partial y^2},\quad \kappa_{xy}=2\frac{\partial^2 w}{\partial y\partial x}.
\end{aligned} \tag{3}$$

In Eq. (3), v, w and u are utilized to represent the mid-plane displacements in y, z and x axes, respectively (Bouderba *et al*. 2013, Zenkour and Sobhy 2013). Using the nonlocal theory (Reddy 2007, Reddy and Pang 2008, Aydogdu 2009, Aydogdu and Arda 2016), the size-dependent basic equation of the kth layer can be written as

$$\begin{aligned}&\left\{\boldsymbol{\sigma}^{(k)}\right\}-\eta_{nl}\nabla^2\left\{\boldsymbol{\sigma}^{(k)}\right\}=\left[\tilde{\mathbf{C}}^{(k)}(\zeta,\phi_k)\right]\left\{\mathbf{e}^0\right\}\\&-z\left[\tilde{\mathbf{C}}^{(k)}(\phi_k,\zeta)\right]\left\{\boldsymbol{\kappa}\right\}+\sigma_{RS}^{(k)}V_{F,k}^{SMA}\left\{\boldsymbol{\mu}\left(\phi_k\right)\right\},\end{aligned} \tag{4}$$

where

$$\left\{\boldsymbol{\sigma}^{(k)}\right\}=\begin{Bmatrix}\sigma_{xx}^{(k)}\\ \sigma_{yy}^{(k)}\\ \sigma_{xy}^{(k)}\end{Bmatrix},\quad \left\{\mathbf{e}^0\right\}=\begin{Bmatrix}e_{xx}^0\\ e_{yy}^0\\ \gamma_{xy}^0\end{Bmatrix},\quad \left\{\boldsymbol{\kappa}\right\}=\begin{Bmatrix}\kappa_{xx}\\ \kappa_{yy}\\ \kappa_{xy}\end{Bmatrix},$$
$$\left\{\boldsymbol{\mu}\left(\phi_k\right)\right\}=\begin{Bmatrix}\mu_1\left(\phi_k\right)\\ \mu_2\left(\phi_k\right)\\ \mu_3\left(\phi_k\right)\end{Bmatrix}=\begin{Bmatrix}\cos^2\left(\phi_k\right)\\ \sin^2\left(\phi_k\right)\\ \cos\left(\phi_k\right)\sin\left(\phi_k\right)\end{Bmatrix}, \tag{5}$$

and

$$\left[\tilde{\mathbf{C}}^{(k)}(\phi_k,\zeta)\right]=\begin{bmatrix}\tilde{C}_{11}^{(k)}(\phi_k,\zeta) & \tilde{C}_{12}^{(k)}(\phi_k,\zeta) & \tilde{C}_{16}^{(k)}(\phi_k,\zeta)\\ \tilde{C}_{12}^{(k)}(\phi_k,\zeta) & \tilde{C}_{22}^{(k)}(\phi_k,\zeta) & \tilde{C}_{26}^{(k)}(\phi_k,\zeta)\\ \tilde{C}_{16}^{(k)}(\phi_k,\zeta) & \tilde{C}_{26}^{(k)}(\phi_k,\zeta) & \tilde{C}_{66}^{(k)}(\phi_k,\zeta)\end{bmatrix}, \tag{6}$$

in which $\eta_{nl} = (e_0a_c)^2$ stands for the scale parameter (Benzair *et al*. 2008, Benguediab *et al*. 2014, Farajpour *et al*. 2018, Zenkour 2018), σ is the stress, a_c and e_0, respectively, represent an internal characteristic dimension and a calibration coefficient (Malekzadeh and Shojaee 2013, Farajpour *et al*. 2017). Also, the elastic constant of the kth plate, nanofiber angle and recovery stresses are indicated by $\widetilde{C_{IJ}^{(k)}}$, ϕ_k and $\sigma_{RS}^{(k)}$, respectively. Finally, ∇^2 is utilized to denote the Laplace operator (Asemi and Farajpour 2014, Zenkour and Sobhy 2015, Farajpour *et al*. 2016). Let us consider n small-scale plates containing nanofibers. The recovery stress resultants and nonlocal stress resultants are

$$\begin{aligned}&\left\{\mathbf{N_{RS}}\right\}=\sum_{l=1}^{n}\int_{z_{l-1}}^{z_l}\sigma_{RS}^{(l)}V_{F,l}^{SMA}\left\{\boldsymbol{\mu}\left(\phi_l\right)\right\}dz,\\&\left\{\mathbf{M_{RS}}\right\}=\sum_{l=1}^{n}\int_{z_{l-1}}^{z_l}\sigma_{RS}^{(l)}V_{F,l}^{SMA}\left\{\boldsymbol{\mu}\left(\phi_l\right)\right\}zdz,\end{aligned} \tag{7}$$

$$\left\{\mathbf{N}\right\}=\sum_{l=1}^{n}\int_{z_{l-1}}^{z_l}\left\{\boldsymbol{\sigma}^{(l)}\right\}dz,\quad \left\{\mathbf{M}\right\}=\sum_{l=1}^{n}\int_{z_{l-1}}^{z_l}\left\{\boldsymbol{\sigma}^{(l)}\right\}zdz, \tag{8}$$

Where

$$\left\{\mathbf{N}\right\}=\begin{Bmatrix}N_{xx}\\ N_{yy}\\ N_{xy}\end{Bmatrix},\quad \left\{\mathbf{M}\right\}=\begin{Bmatrix}M_{xx}\\ M_{yy}\\ M_{xy}\end{Bmatrix}, \tag{9}$$
$$\left\{\mathbf{N_{RS}}\right\}=\begin{Bmatrix}N_{xx}^{RS}\\ N_{yy}^{RS}\\ N_{xy}^{RS}\end{Bmatrix},\quad \left\{\mathbf{M_{RS}}\right\}=\begin{Bmatrix}M_{xx}^{RS}\\ M_{yy}^{RS}\\ M_{xy}^{RS}\end{Bmatrix},$$

In view of the above equations (i.e. Eqs. (4)-(9)), one obtains the recovery stress resultants and nonlocal stress resultants as follows

$$\left\{\mathbf{N}\right\}-\eta_{nl}\nabla^2\left\{\mathbf{N}\right\}=\left[\tilde{\mathbf{K}}\right]\left\{\mathbf{e}^0\right\}-\left[\tilde{\mathbf{F}}\right]\left\{\boldsymbol{\kappa}\right\}+\left\{\mathbf{N_{RS}}\right\}, \tag{10}$$

$$\left\{\mathbf{M}\right\}-\eta_{nl}\nabla^2\left\{\mathbf{M}\right\}=\left[\tilde{\mathbf{F}}\right]\left\{\mathbf{e}^0\right\}-\left[\tilde{\mathbf{S}}\right]\left\{\boldsymbol{\kappa}\right\}+\left\{\mathbf{M_{RS}}\right\}, \tag{11}$$

where

$$\begin{aligned}&\left[\tilde{\mathbf{K}}\right]=\begin{bmatrix}\tilde{K}_{11} & \tilde{K}_{12} & \tilde{K}_{16}\\ \tilde{K}_{12} & \tilde{K}_{22} & \tilde{K}_{26}\\ \tilde{K}_{16} & \tilde{K}_{26} & \tilde{K}_{66}\end{bmatrix},\\&\left[\tilde{\mathbf{S}}\right]=\begin{bmatrix}\tilde{S}_{11} & \tilde{S}_{12} & \tilde{S}_{16}\\ \tilde{S}_{12} & \tilde{S}_{22} & \tilde{S}_{26}\\ \tilde{S}_{16} & \tilde{S}_{26} & \tilde{S}_{66}\end{bmatrix},\\&\left[\tilde{\mathbf{F}}\right]=\begin{bmatrix}\tilde{F}_{11} & \tilde{F}_{12} & \tilde{F}_{16}\\ \tilde{F}_{12} & \tilde{F}_{22} & \tilde{F}_{26}\\ \tilde{F}_{16} & \tilde{F}_{26} & \tilde{F}_{66}\end{bmatrix},\end{aligned} \tag{12}$$

and

$$\begin{aligned}&\tilde{K}_{ij}=\sum_{l=1}^{n}\tilde{C}_{ij}^{(l)}\left(z_l-z_{l-1}\right),\\&\tilde{F}_{ij}=\frac{1}{2}\sum_{l=1}^{n}\tilde{C}_{ij}^{(l)}\left(z_l^2-z_{l-1}^2\right),\\&\tilde{S}_{ij}=\frac{1}{3}\sum_{l=1}^{n}\tilde{C}_{ij}^{(l)}\left(z_l^3-z_{l-1}^3\right).\end{aligned} \tag{13}$$

The motion equations of the small-scale system in terms of nonlocal stress resultants are as

$$\frac{\partial N_{xx}}{\partial x}+\frac{\partial N_{xy}}{\partial y}-m_{sys}\frac{\partial^2 u}{\partial t^2}=0, \tag{14}$$

$$\frac{\partial N_{xy}}{\partial x}+\frac{\partial N_{yy}}{\partial y}-m_{sys}\frac{\partial^2 v}{\partial t^2}=0, \tag{15}$$

$$\begin{aligned}&\frac{\partial^2 M_{xx}}{\partial x^2}+2\frac{\partial^2 M_{xy}}{\partial x\partial y}+\frac{\partial^2 M_{yy}}{\partial y^2}+\frac{\partial}{\partial y}\left(N_{xy}\frac{\partial w}{\partial x}+N_{yy}\frac{\partial w}{\partial y}\right)\\&+\frac{\partial}{\partial x}\left(N_{xx}\frac{\partial w}{\partial x}+N_{xy}\frac{\partial w}{\partial y}\right)+q_{em}-m_{sys}\frac{\partial^2 w}{\partial t^2}=0.\end{aligned} \tag{16}$$

Here q_{em} and m_{sys} are respectively the distributed load induced by the elastic matrix and the system mass per unit area. The distributed load can be expressed as (Akgöz and Civalek 2017, Akgöz and Civalek 2018)

$$q_{em} = -k_n w + k_s \frac{\partial^2 w}{\partial y^2} + k_s \frac{\partial^2 w}{\partial x^2}. \qquad (17)$$

Equation (17) is in consistent with the equation of the elastic medium reported in the literature (Beldjelili *et al*. 2016, Bounouara *et al*. 2016, Attia *et al*. 2018, Kadari *et al*. 2018). Substituting Eqs. (10), (11) and (17) into Eqs. (14)-(16), the differential equations for the elastic wave dispersion in the system are derived as

$$\begin{aligned}&\tilde{K}_{11}\frac{\partial^2 u}{\partial x^2} + \tilde{K}_{66}\frac{\partial^2 u}{\partial y^2} + 2\tilde{K}_{16}\frac{\partial^2 u}{\partial y \partial x} + \left(\tilde{K}_{66} + \tilde{K}_{12}\right)\frac{\partial^2 v}{\partial y \partial x}\\ &+\tilde{K}_{16}\frac{\partial^2 v}{\partial x^2} + \tilde{K}_{26}\frac{\partial^2 v}{\partial y^2} - \left(\tilde{F}_{11}\frac{\partial^3 w}{\partial x^3} + \left(\tilde{F}_{12} + 2\tilde{F}_{66}\right)\frac{\partial^3 w}{\partial y^2 \partial x}\right.\\ &\left.+3\tilde{F}_{16}\frac{\partial^3 w}{\partial y \partial x^2} + \tilde{F}_{26}\frac{\partial^3 w}{\partial y^3}\right) = m_{sys}\frac{\partial^2 u}{\partial t^2} - m_{sys}\eta_{nl}\nabla^2\frac{\partial^2 u}{\partial t^2},\end{aligned} \qquad (18)$$

$$\begin{aligned}&\tilde{K}_{16}\frac{\partial^2 u}{\partial x^2} + \tilde{K}_{26}\frac{\partial^2 u}{\partial y^2} + \left(\tilde{K}_{66} + \tilde{K}_{12}\right)\frac{\partial^2 u}{\partial y \partial x}\\ &+\tilde{K}_{66}\frac{\partial^2 v}{\partial x^2} + \tilde{K}_{22}\frac{\partial^2 v}{\partial y^2} + 2\tilde{K}_{26}\frac{\partial^2 v}{\partial y \partial x}\\ &-\left(\tilde{F}_{16}\frac{\partial^3 w}{\partial x^3} + 3\tilde{F}_{26}\frac{\partial^3 w}{\partial y^2 \partial x} + \left(\tilde{F}_{12} + 2\tilde{F}_{66}\right)\frac{\partial^3 w}{\partial y \partial x^2} + \tilde{F}_{22}\frac{\partial^3 w}{\partial y^3}\right)\\ &= m_{sys}\frac{\partial^2 v}{\partial t^2} - m_{sys}\eta_{nl}\nabla^2\frac{\partial^2 v}{\partial t^2},\end{aligned} \qquad (19)$$

$$\begin{aligned}&\tilde{F}_{11}\frac{\partial^3 u}{\partial x^3} + \tilde{F}_{26}\frac{\partial^3 u}{\partial y^3} + 3\tilde{F}_{16}\frac{\partial^3 u}{\partial y \partial x^2}\\ &+\left(2\tilde{F}_{66} + \tilde{F}_{12}\right)\frac{\partial^3 u}{\partial x \partial y^2} + \tilde{F}_{16}\frac{\partial^3 v}{\partial x^3} +\\ &\tilde{F}_{22}\frac{\partial^3 v}{\partial y^3} + \left(2\tilde{F}_{66} + \tilde{F}_{12}\right)\frac{\partial^3 v}{\partial y \partial x^2} + 3\tilde{F}_{26}\frac{\partial^3 v}{\partial y^2 \partial x}\\ &-\left(\tilde{S}_{11}\frac{\partial^4 w}{\partial x^4} + \tilde{S}_{22}\frac{\partial^4 w}{\partial y^4} + 2\left(2\tilde{S}_{66} + \tilde{S}_{12}\right)\frac{\partial^4 w}{\partial y^2 \partial x^2} + 4\tilde{S}_{16}\frac{\partial^4 w}{\partial y \partial x^3}\right.\\ &\left.+4\tilde{S}_{26}\frac{\partial^4 w}{\partial x \partial y^3}\right) + N_{xx}^{RS}\frac{\partial^2 w}{\partial x^2} + N_{yy}^{RS}\frac{\partial^2 w}{\partial y^2}\\ &+2\left(N_{xy}^{RS} + N_{xy}^{SP}\right)\frac{\partial^2 w}{\partial x \partial y}\\ &-\mu_{nl}\left(N_{xx}^{RS}\frac{\partial^4 w}{\partial x^4} + N_{yy}^{RS}\frac{\partial^4 w}{\partial y^4} + 2\left(N_{xy}^{RS} + N_{xy}^{SP}\right)\frac{\partial^4 w}{\partial x^3 \partial y}\right.\\ &\left.+\left(N_{xx}^{RS} + N_{yy}^{RS}\right)\frac{\partial^4 w}{\partial y^2 \partial x^2} + 2\left(N_{xy}^{RS} + N_{xy}^{SP}\right)\frac{\partial^4 w}{\partial x \partial y^3}\right)\\ &-k_n w + k_n\eta_{nl}\left(\frac{\partial^2 w}{\partial y^2} + \frac{\partial^2 w}{\partial x^2}\right) + k_s\left(\frac{\partial^2 w}{\partial y^2} + \frac{\partial^2 w}{\partial x^2}\right)\\ &-k_s\eta_{nl}\left(\frac{\partial^4 w}{\partial y^4} + 2\frac{\partial^4 w}{\partial x^2 \partial y^2} + \frac{\partial^4 w}{\partial x^4}\right) = m_{sys}\frac{\partial^2 w}{\partial t^2} - m_{sys}\eta_{nl}\nabla^2\frac{\partial^2 w}{\partial t^2}.\end{aligned} \qquad (20)$$

More detail about the derivation of the above equations is given in Appendix B. N_{xy}^{SP} denotes the shear preload. N_{xy}^{SP} is related to the shear initial stress ($\sigma_{xy(l)}^0$) by the following relation

$$N_{xy}^{SP} = \sum_{l=1}^{n}\int_{z_{l-1}}^{z_l}\sigma_{xy(l)}^0 dz. \qquad (21)$$

The following expressions are assumed for the displacement components of the small-scale system containing nanofibers so as to extract the phase and group velocities (Ebrahimi *et al*. 2016)

$$\begin{aligned}u(x,y,t) &= \hat{A}\exp\left(-i\omega t + ik_y y + ik_x x\right),\\ v(x,y,t) &= \hat{B}\exp\left(-i\omega t + ik_y y + ik_x x\right),\\ w(x,y,t) &= \hat{C}\exp\left(-i\omega t + ik_y y + ik_x x\right),\end{aligned} \qquad (22)$$

where k_x and k_y are, respectively, utilized to indicate the wave numbers in longitudinal and width directions, $\hat{A}$, $\hat{B}$ and $\hat{C}$ represent wave amplitude constants, also, ω denotes the system frequency. Substituting Eq. (22) into Eqs. (18)-(20) yields

$$[\tilde{\Sigma}]\{\Delta\} - \omega^2[\tilde{\Gamma}]\{\Delta\} = 0, \qquad (23)$$

where

$$\left[\tilde{\mathbf{\Sigma}}\right] = \begin{bmatrix}\tilde{\Sigma}_{11} & \tilde{\Sigma}_{12} & \tilde{\Sigma}_{13}\\ \tilde{\Sigma}_{21} & \tilde{\Sigma}_{22} & \tilde{\Sigma}_{23}\\ \tilde{\Sigma}_{31} & \tilde{\Sigma}_{32} & \tilde{\Sigma}_{33}\end{bmatrix},\quad \left[\tilde{\mathbf{\Gamma}}\right] = \begin{bmatrix}\tilde{\Gamma}_{11} & \tilde{\Gamma}_{12} & \tilde{\Gamma}_{13}\\ \tilde{\Gamma}_{21} & \tilde{\Gamma}_{22} & \tilde{\Gamma}_{23}\\ \tilde{\Gamma}_{31} & \tilde{\Gamma}_{32} & \tilde{\Gamma}_{33}\end{bmatrix},\quad \left\{\hat{\mathbf{\Delta}}\right\} = \begin{Bmatrix}\hat{A}\\ \hat{B}\\ \hat{C}\end{Bmatrix}. \qquad (24)$$

The size-dependent dispersion relation for the small-scale system containing nanofibers is expressed as

$$\left|\left[\tilde{\mathbf{\Sigma}}\right] - \omega^2\left[\tilde{\mathbf{\Gamma}}\right]\right| = 0. \qquad (25)$$

In Eq. (25), "| |" is the determinant of a matrix. Assuming that the wave numbers in longitudinal and width directions are the same (k=k_x=k_y), we have $K = \sqrt{k_k^2 + k_y^2} = \sqrt{2}k$ in which K is the general wave number. The phase and group velocities are obtained as

$$c_p = \frac{\omega}{K}, \qquad (26)$$

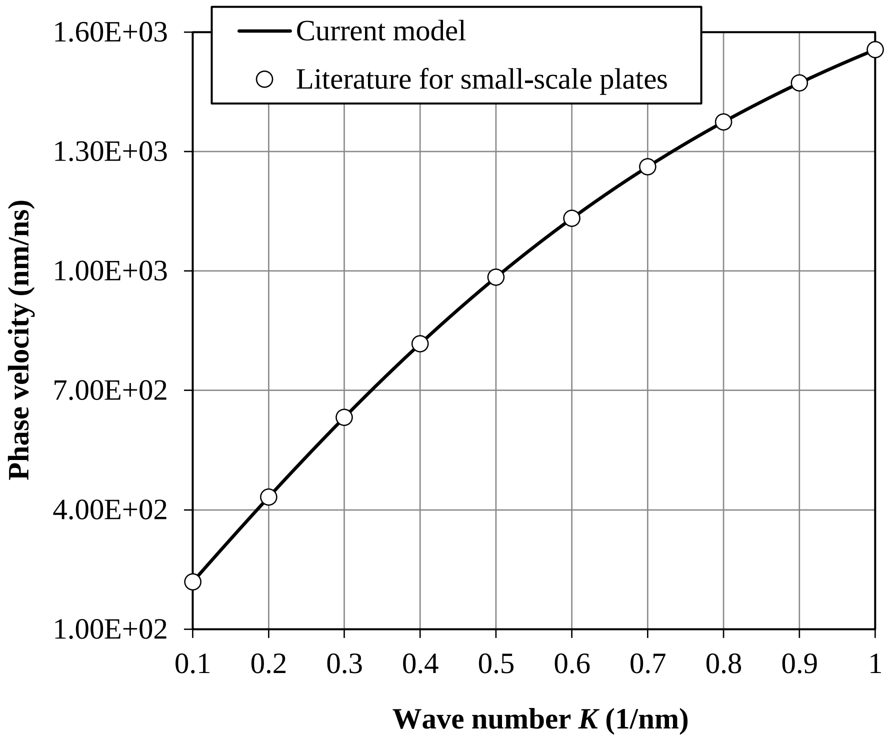

Fig. 2 Phase velocities of the current model in comparison with literature data (Wang *et al*. 2010)

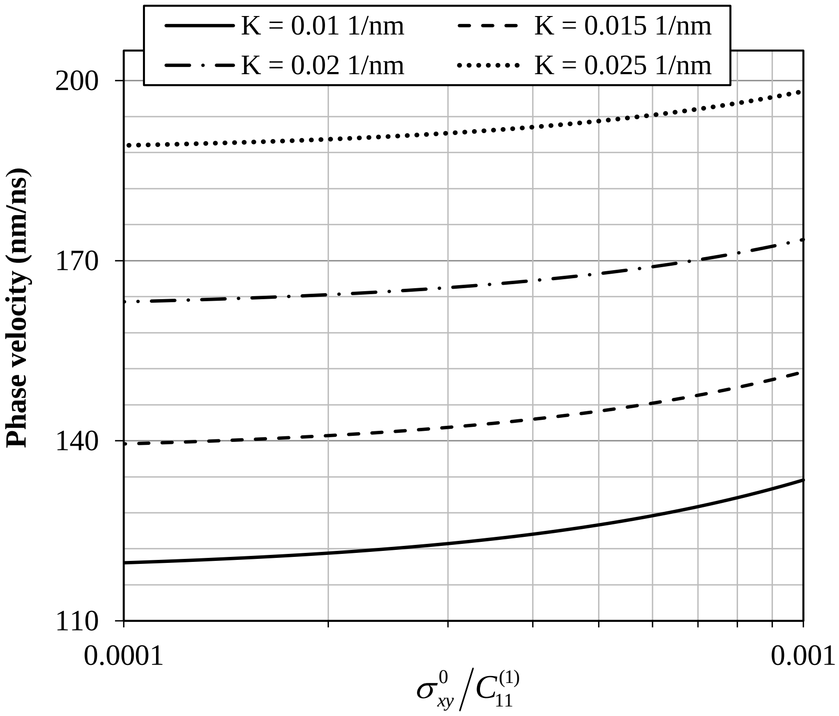

Fig. 3 Influences of shear in-plane preload on the phase velocity of the plate containing nanofibers

$$c_g = \frac{d\omega}{dK}. \tag{27}$$

Here the group velocity is indicated by c_g while c_p denotes the phase velocity of the small-scale system containing nanofibers

3. Results and discussion

For comparison purposes, the variation of phase velocities with the wave number is plotted in Fig. 2, the results are compared with those extracted by Wang *et al*. (Wang *et al*. 2010) for small-scale plates. To make a

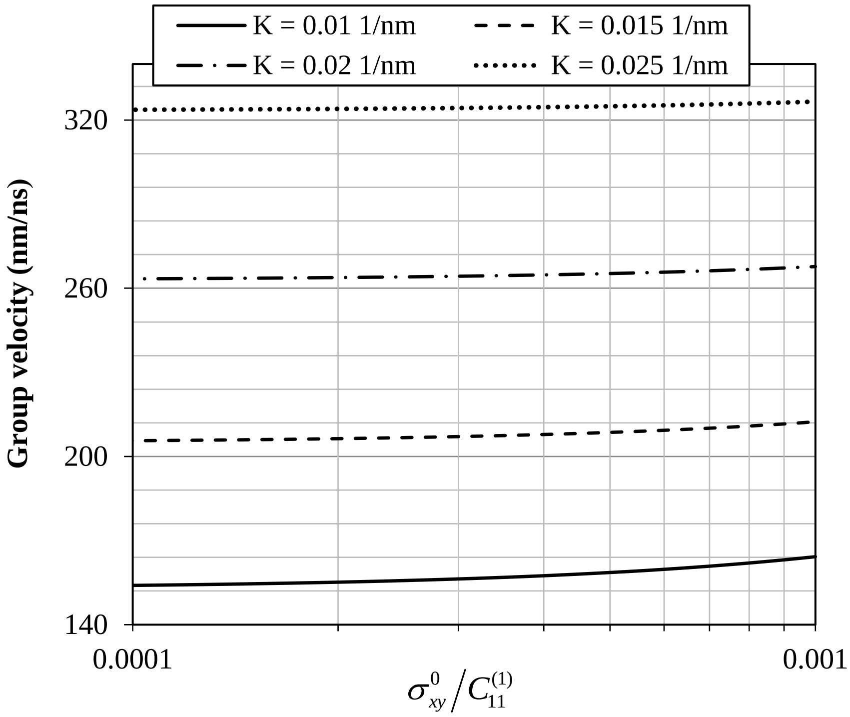

Fig. 4 Influences of shear in-plane preload on the group velocity of the plate containing nanofibers

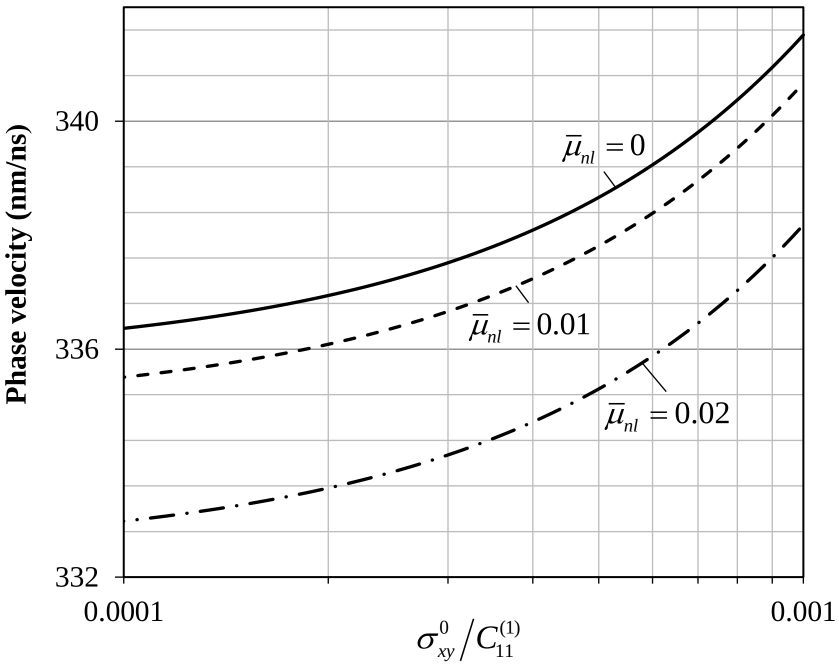

Fig. 5 Influences of scale parameter and shear preload on the phase velocity of the plate containing nanofibers

reasonable comparison, nanofiber effects are ignored in this figure. For the ultrasmall plate, we assume that the plate thickness and nonlocal parameter are 0.34 and 1 nm, respectively. Furthermore, the density, Poisson's ratio and elasticity modulus are chosen as 2250 kg/m^3, 0.25, 1.06 TPa, respectively (Wang *et al.* 2010). An excellent agreement is seen between the results and those available in the literature.

Figures 3 and 4 indicate the influences of shear prestress on the phase and group velocities of the small-scale plate containing nanofibers. The shear in-plane preload is assumed to be uniform. The nanoscale system consists of

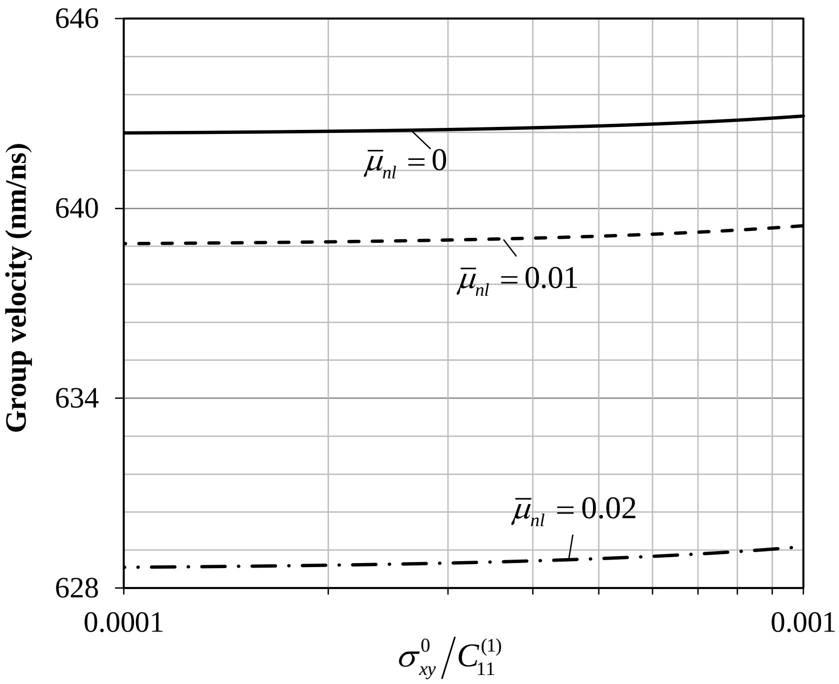

Fig. 6 Influences of scale parameter and shear preload on the group velocity of the plate containing nanofibers

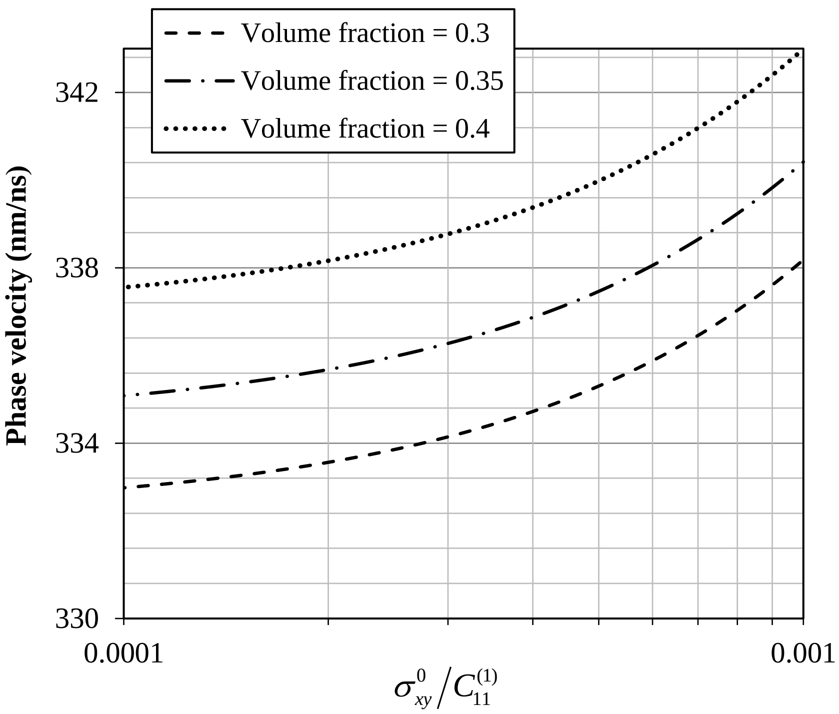

Fig. 7 Influences of volume fraction and shear preload on the phase velocity of the plate containing nanofibers

five plates containing nanofibers with the same material properties (ν_F=0.3, ρ_F =6450 kg/m^3, σ_{RS} =0.2 GPa, E_F=30 GPa, V_F=0.3, and ϕ =0^0 for nanofibers; ν_L=0.3, ρ_L =1600 kg/m^3 and E_L=3.44 GPa for each plate (Farajpour *et al.* 2018)). Each layer's aspect ratio, length and thickness are 1, 150 nm and 3 nm, respectively. The elastic medium is not taken into consideration. The nonlocal parameter-to-length ratio is considered as 0.02. From the results given in Fig. 3, it is seen that the phase velocity of small-scale plates is greater for greater values of shear prestress. In addition, the shear in-plane preload affects the group velocity. Greater values of shear preload result in slightly greater

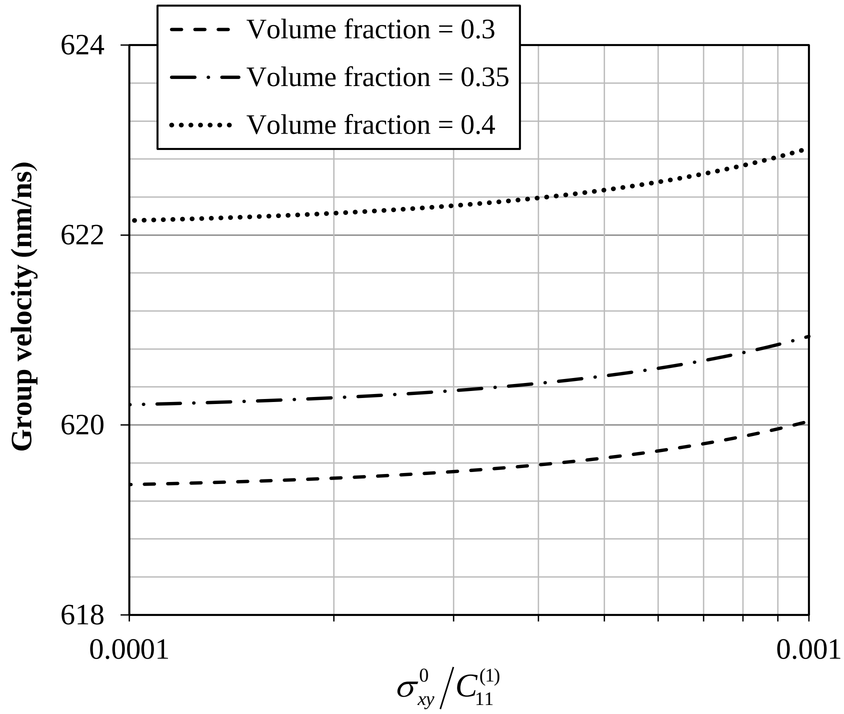

Fig. 8 Influences of volume fraction and shear preload on the group velocity of the plate containing nanofibers

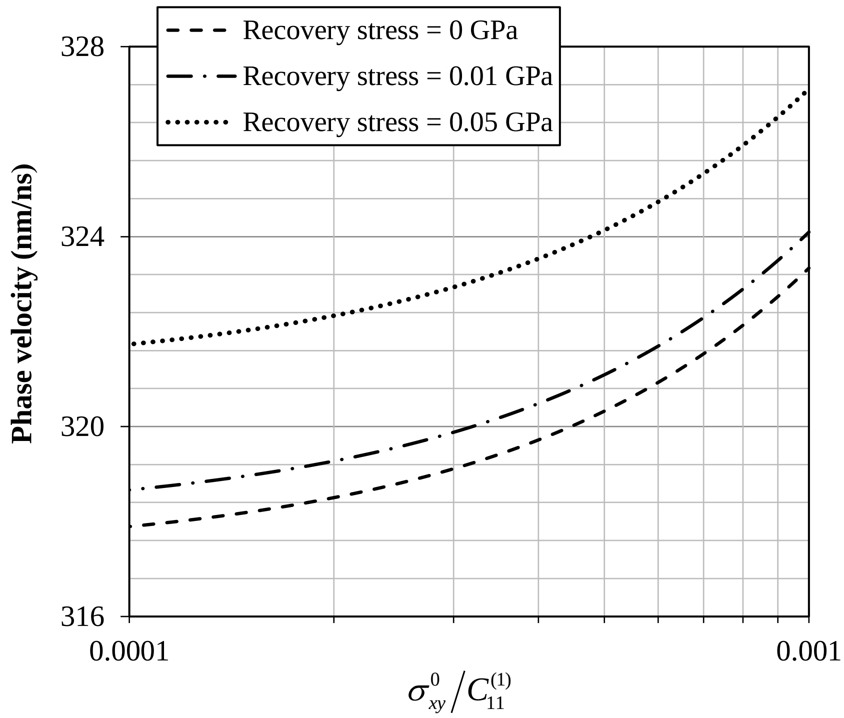

Fig. 9 Influences of recovery stress and shear preload on the phase velocity of the plate containing nanofibers

group velocities.

The influences of shear in-plane preload together with scale influences are indicated in Figs. 5 and 6. The total wave number is 0.05 1/nm. The elastic medium is not taken into consideration. Stronger scale effects yield lower group and phase velocities. It is rooted in the fact that stronger scale effects correspond to a lower total stiffness for the small-scale system; consequently, lower values of structural stiffness lead to lower frequencies. From Eq. (26), it can be seen that lower frequencies result in lower phase velocities.

Figures 7 and 8, respectively, depict the effects of shear prestress and volume fraction on the phase and group

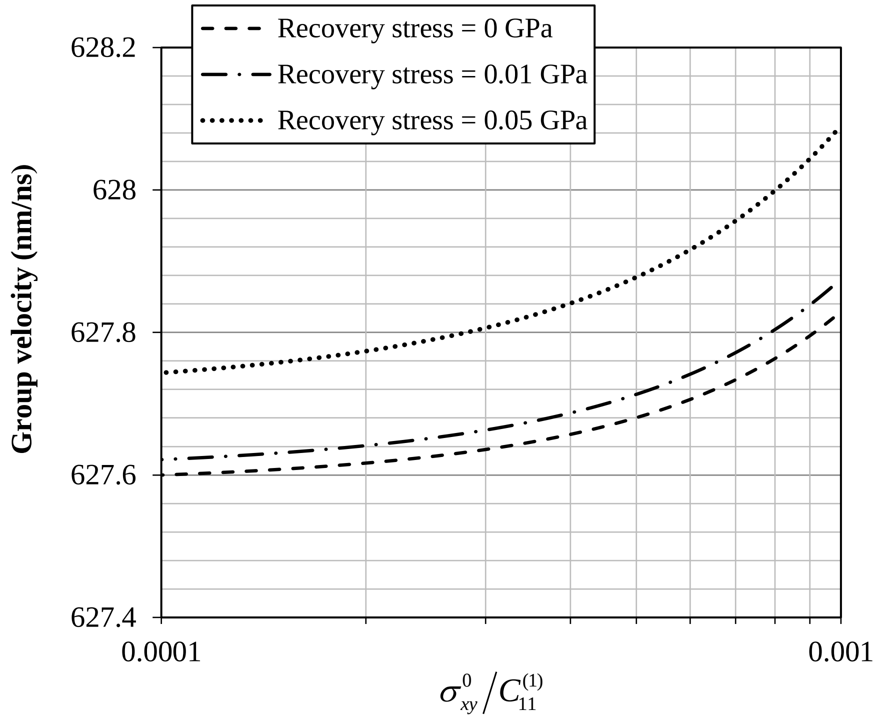

Fig. 10 Influences of recovery stress and shear preload on the group velocity of the plate containing nanofibers

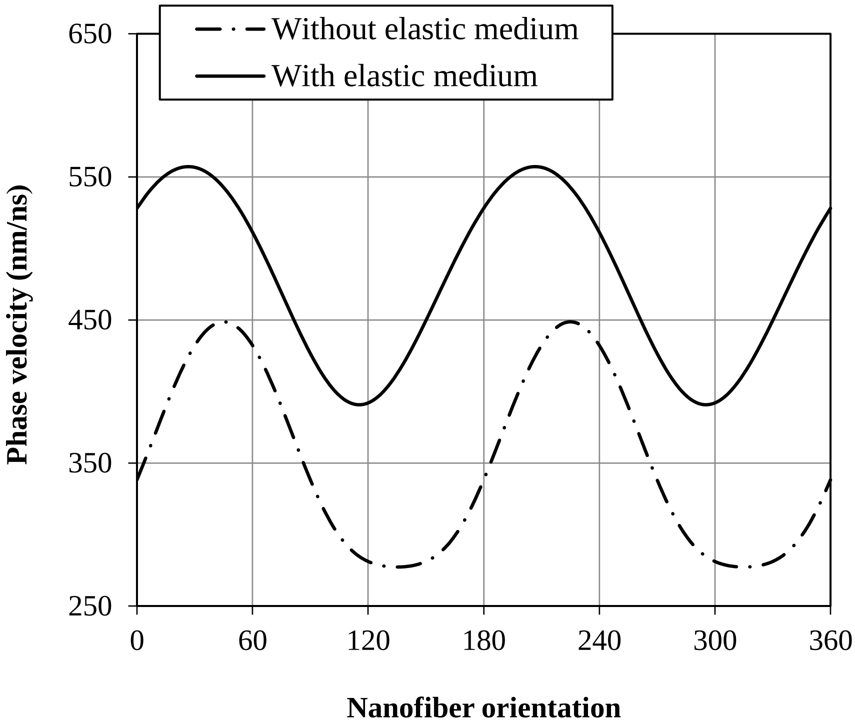

Fig. 11 Influences of elastic medium on the phase velocity of the plate containing nanofibers $\sigma^0_{xy}/C^{(1)}_{11} = 0.001$

velocities of the small-scale plate containing nanofibers. The dimensionless scale parameter and total wave number are, respectively, given by 0.02 and 0.05 1/nm. Generally, greater volume fractions yield greater phase and group velocities. This is because increasing the volume fraction of nanofibers increases the stiffness of the composite structure.

To understand the influence of recovery stress on the phase and group velocities of small-scale plates containing nanofibers, Figs. 9 and 10 are plotted. The dimensionless scale parameter, total wave number and volume fraction are, respectively, given by 0.02, 0.05 1/nm and 0.3. Comparing Figs. 7 and 8 with Figs. 9 and 10, one can conclude that the wave propagation characteristics, especially the group velocity, are less sensitive to the

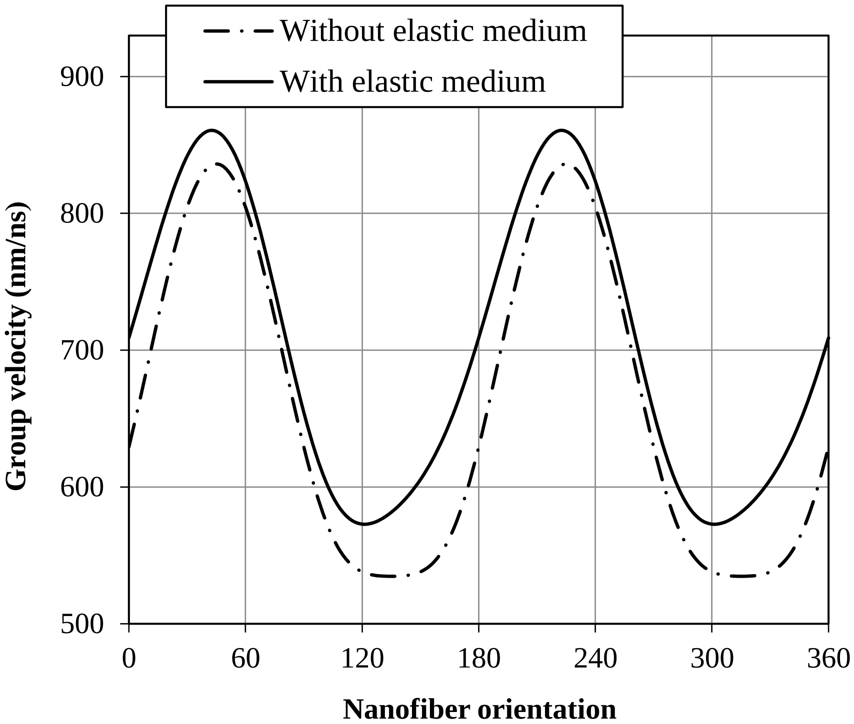

Fig. 12 Influences of elastic medium on the group velocity of the plate containing nanofibers $\sigma_{xy}^0/C_{11}^{(1)} = 0.001$

recovery stress in comparison with the volume fraction. Nevertheless, the phase and group velocities for nanofibers with high recovery stresses are higher than those for small recovery stresses.

Figure 11 is plotted to illustrate the influence of elastic medium on the phase velocity while Fig. 12 is aimed at illustrating the influence of elastic medium on the group velocity. The dimensionless scale parameter, total wave number, volume fraction and recovery stress are, respectively, given by 0.02, 0.05 1/nm, 0.3 and 0.2 GPa. The normal and shear stiffness coefficients of the elastic medium are $k_n a^4/\tilde{S}_{11} = 50$ and $k_s a^2/\tilde{S}_{11} = 50$, respectively. It can be concluded that the phase and group velocities are enhanced when the small-scale plate is embedded in an elastic medium. This is due to the fact that utilizing an elastic medium increases the total structural stiffness of the system, and this consequently increases the value of phase and group velocities.

4. Conclusions

The effects of shear in-plane preload on the wave propagation response of small-scale plate containing nanofibers were explored. To develop a more realistic model, the small-scale system was assumed to be embedded in an elastic matrix. A size-dependent model of plates was proposed for the problem via nonlocal elasticity. The size-dependent differential equations were derived for motions along all directions. The differential equations were analytically solved so as to extract the phase and group velocities of the plate subjected to shear preload. The present results indicated that the phase velocity of small-scale plates containing nanofibers is greater for greater values of shear preload. Furthermore, greater values of shear preload result in slightly greater group velocities. It was also indicated that stronger scale effects yield lower group and phase velocities. The wave propagation characteristics are more sensitive to the volume fraction in comparison with the recovery stress. Moreover, as the plate is embedded in an elastic medium, both phase and group velocities are enhanced.

References

Ahouel, M., Houari, M.S.A., Bedia, E. and Tounsi, A. (2016), "Size-dependent mechanical behavior of functionally graded trigonometric shear deformable nanobeams including neutral surface position concept", *Steel Compos. Struct.*, **20**(5), 963-981. http://doi.org/10.12989/scs.2016.20.5.963

Akgöz, B. and Civalek, Ö. (2013), "Modeling and analysis of micro-sized plates resting on elastic medium using the modified couple stress theory", *Meccanica*, 48(4), 863-873. https://doi.org/10.1007/s11012-012-9639-x

Akgöz, B. and Civalek, Ö. (2017), "A size-dependent beam model for stability of axially loaded carbon nanotubes surrounded by Pasternak elastic foundation", *Compos. Struct.*, **176**, 1028-1038. https://doi.org/10.1016/j.compstruct.2017.06.039

Akgöz, B. and Civalek, Ö. (2018), "Vibrational characteristics of embedded microbeams lying on a two-parameter elastic foundation in thermal environment", *Compos. Part B*, **150**, 68-77. https://doi.org/10.1016/j.compositesb.2018.05.049

Aksencer, T. and Aydogdu, M. (2011), "Levy type solution method for vibration and buckling of nanoplates using nonlocal elasticity theory", *Physica E*, **43**(4), 954-959. https://doi.org/10.1016/j.physe.2010.11.024.

Asemi, S., Farajpour, A., Asemi, H. and Mohammadi, M. (2014), "Influence of initial stress on the vibration of double-

piezoelectric-nanoplate systems with various boundary conditions using DQM", *Physica E*, **63**, 169-179. https://doi.org/10.1016/j.physe.2014.05.009
Asemi, S.R. and Farajpour, A. (2014), "Vibration characteristics of double-piezoelectric-nanoplate-systems", *IET Micro Nano Lett.,* **9**(4), 280-285. https://doi.org/10.1049/mnl.2013.0741.
Asemi, S.R., Farajpour, A., Borghei, M. and Hassani, A.H. (2014), "Thermal effects on the stability of circular graphene sheets via nonlocal continuum mechanics", *Latin American J. Solids Struct.*, **11**(4), 704-724. http://doi.org/10.1590/S1679-78252014000400009
Attia, A., Bousahla, A.A., Tounsi, A., Mahmoud, S. and Alwabli, A.S. (2018), "A refined four variable plate theory for thermoelastic analysis of FGM plates resting on variable elastic foundations", *Struct. Eng. Mech.*, **65**(4), 453-464. https://doi.org/10.12989/sem.2018.65.4.453
Aydogdu, M. (2009), "A general nonlocal beam theory: its application to nanobeam bending, buckling and vibration", *Physica E*, **41**(9), 1651-1655. https://doi.org/10.1016/j.physe.2009.05.014
Aydogdu, M. and Arda, M. (2016), "Torsional vibration analysis of double walled carbon nanotubes using nonlocal elasticity", *J. Mech. Mater. Design*, **12**(1), 71-84. https://doi.org/10.1007/s10999-014-9292-8.
Bakhadda, B., Bouiadjra, M.B., Bourada, F., Bousahla, A.A., Tounsi, A. and Mahmoud, S. (2018), "Dynamic and bending analysis of carbon nanotube-reinforced composite plates with elastic foundation", *Wind Struct.*, **27**(5), 311-324. https://doi.org/10.12989/was.2018.27.5.311.
Beldjelili, Y., Tounsi, A. and Mahmoud, S. (2016), "Hygro-thermo-mechanical bending of S-FGM plates resting on variable elastic foundations using a four-variable trigonometric plate theory", *Smart Struct. Syst.*, **18**(4), 755-786. http://doi.org/10.12989/sss.2016.18.4.755.
Belkorissat, I., Houari, M.S.A., Tounsi, A., Bedia, E. and Mahmoud, S. (2015), "On vibration properties of functionally graded nano-plate using a new nonlocal refined four variable model", *Steel Compos. Struct*, **18**(4), 1063-1081. http://doi.org/10.12989/scs.2015.18.4.1063.
Bellifa, H., Benrahou, K.H., Bousahla, A.A., Tounsi, A. and Mahmoud, S. (2017), "A nonlocal zeroth-order shear deformation theory for nonlinear postbuckling of nanobeams", *Struct. Eng. Mech.*, **62**(6), 695-702. http://doi.org/10.12989/sem.2017.62.6.695.
Benguediab, S., Tounsi, A., Zidour, M. and Semmah, A. (2014), "Chirality and scale effects on mechanical buckling properties of zigzag double-walled carbon nanotubes", *Compos. Part B*, **57**, 21-24. https://doi.org/10.1016/j.compositesb.2013.08.020.
Benzair, A., Tounsi, A., Besseghier, A., Heireche, H., Moulay, N. and Boumia, L. (2008), "The thermal effect on vibration of single-walled carbon nanotubes using nonlocal Timoshenko beam theory", *J. Physics D*, **41**(22), 225404. https://doi.org/10.1016/j.commatsci.2011.07.021.
Besseghier, A., Houari, M.S.A., Tounsi, A. and Mahmoud, S. (2017), "Free vibration analysis of embedded nanosize FG plates using a new nonlocal trigonometric shear deformation theory", *Smart Struct. Syst*, **19**(6), 601-614. https://doi.org/10.12989/sss.2017.19.6.601.
Bouadi, A., Bousahla, A.A., Houari, M.S.A., Heireche, H. and Tounsi, A. (2018), "A new nonlocal HSDT for analysis of stability of single layer graphene sheet", *Adv. Nano Res.*, **6**(2), 147-162. https://doi.org/10.12989/anr.2018.6.2.147.
Bouafia, K., Kaci, A., Houari, M.S.A., Benzair, A. and Tounsi, A. (2017), "A nonlocal quasi-3D theory for bending and free flexural vibration behaviors of functionally graded nanobeams", *Smart Struct. Syst*, **19**(2), 115-126. https://doi.org/10.12989/sss.2017.19.2.115.
Bouderba, B., Houari, M.S.A. and Tounsi, A. (2013), "Thermomechanical bending response of FGM thick plates resting on Winkler-Pasternak elastic foundations", *Steel Compos. Struct.*, **14**(1), 85-104.
Bounouara, F., Benrahou, K.H., Belkorissat, I. and Tounsi, A. (2016), "A nonlocal zeroth-order shear deformation theory for free vibration of functionally graded nanoscale plates resting on elastic foundation", *Steel Compos. Struct.*, **20**(2), 227-249.
Brinson, L.C. (1993), "One-dimensional constitutive behavior of shape memory alloys: thermomechanical derivation with non-constant material functions and redefined martensite internal variable", Journal of intelligent material systems and structures, **4**(2), 229-242.
Chaht, F.L., Kaci, A., Houari, M.S.A., Tounsi, A., Bég, O.A. and Mahmoud, S. (2015), "Bending and buckling analyses of functionally graded material (FGM) size-dependent nanoscale beams including the thickness stretching effect", *Steel Compos. Struct.*, **18**(2), 425-442. https://doi.org/10.12989/scs.2015.18.2.425
Chakraverty, S. and Behera, L. (2015), "Small scale effect on the vibration of non-uniform nanoplates", *Struct. Eng. Mech.*, **55**(3), 495-510. http://doi.org/10.12989/sem.2015.55.3.495
Civalek, Ö. (2013), "Nonlinear dynamic response of laminated plates resting on nonlinear elastic foundations by the discrete singular convolution-differential quadrature coupled approaches", *Compos. Part B*, **50**, 171-179. https://doi.org/10.1016/j.compositesb.2013.01.027
Ebrahimi, F. and Barati, M.R. (2018), "A nonlocal strain gradient refined plate model for thermal vibration analysis of embedded graphene sheets via DQM", *Struct. Eng. Mech.*, **66**(6), 693-701. https://doi.org/10.12989/sem.2018.66.6.693
Ebrahimi, F. and Barati, M.R. (2018), "Surface and flexoelectricity effects on size-dependent thermal stability analysis of smart piezoelectric nanoplates", *Struct. Eng. Mech.*, **67**(2), 143-153. https://doi.org/10.12989/sem.2018.67.2.143
Ebrahimi, F. and Barati, M.R. (2018), "A unified formulation for modeling of inhomogeneous nonlocal beams", *Struct. Eng. Mech.*, **66**(3), 369-377. https://doi.org/10.12989/sem.2018.66.3.369
Ebrahimi, F. and Barati, M.R. (2018), "Wave propagation analysis of smart strain gradient piezo-magneto-elastic nonlocal beams", *Struct. Eng. Mech.*, **66**(2), 237-248. https://doi.org/10.12989/sem.2018.66.2.237
Ebrahimi, F., Barati, M.R. and Dabbagh, A. (2016), "A nonlocal strain gradient theory for wave propagation analysis in temperature-dependent inhomogeneous nanoplates", *J. Eng. Sci.*, **107**, 169-182. https://doi.org/10.1016/j.ijengsci.2016.07.008
Ebrahimi, F. and Heidari, E. (2018), "Vibration characteristics of advanced nanoplates in humid-thermal environment incorporating surface elasticity effects via differential quadrature method", *Struct. Eng. Mech..*, **68**(1), 131-157. http://doi.org/10.12989/sem.2018.68.1.131
Ebrahimi, F. and Shafiei, N. (2017), "Influence of initial shear stress on the vibration behavior of single-layered graphene sheets embedded in an elastic medium based on Reddy's higher-order shear deformation plate theory", *Mech. Adv. Mater. Struct.*, **24**(9), 761-772. https://doi.org/10.1080/15376494.2016.1196781
Farajpour, A. and Rastgoo, A. (2017), "Influence of carbon nanotubes on the buckling of microtubule bundles in viscoelastic cytoplasm using nonlocal strain gradient theory", *Results Phys.*, **7**, 1367-1375. https://doi.org/10.1016/j.rinp.2017.03.038
Farajpour, A. and Rastgoo, A. (2017), "Size-dependent static stability of magneto-electro-elastic CNT/MT-based composite nanoshells under external electric and magnetic fields",

Microsyst. Technol., **23**(12), 5815-5832. https://doi.org/10.1007/s00542-017-3440-7.

Farajpour, A., Rastgoo, A. and Farajpour, M. (2017), "Nonlinear buckling analysis of magneto-electro-elastic CNT-MT hybrid nanoshells based on the nonlocal continuum mechanics", *Compos. Struct.*, **180**, 179-191. https://doi.org/10.1016/j.compstruct.2017.07.100.

Farajpour, A., Rastgoo, A. and Mohammadi, M. (2014), "Surface effects on the mechanical characteristics of microtubule networks in living cells", *Mech. Res. Communications*, **57**, 18-26. https://doi.org/10.1016/j.mechrescom.2014.01.005.

Farajpour, A., Rastgoo, A. and Mohammadi, M. (2017), "Vibration, buckling and smart control of microtubules using piezoelectric nanoshells under electric voltage in thermal environment", *Physica B*, **509**, 100-114. https://doi.org/10.1016/j.physb.2017.01.006.

Farajpour, M., Shahidi, A. and Farajpour, A. (2018), "A nonlocal continuum model for the biaxial buckling analysis of composite nanoplates with shape memory alloy nanowires", *Mater. Res. Exp.*, **5**(3), 035026.

Farajpour, M., Shahidi, A., Hadi, A. and Farajpour, A. (2018), "Influence of initial edge displacement on the nonlinear vibration, electrical and magnetic instabilities of magneto-electro-elastic nanofilms", *Mech. Adv. Mater. Struct.*, http://doi.org/10.1080/15376494.2018.1432820.

Farajpour, M., Shahidi, A., Tabataba'i-Nasab, F. and Farajpour, A. (2018), "Vibration of initially stressed carbon nanotubes under magneto-thermal environment for nanoparticle delivery via higher-order nonlocal strain gradient theory", *European Phys. J. Plus*, **133**(6), 219. https://doi.org/10.1140/epjp/i2018-12039-5.

Farajpour, M.R., Rastgoo, A., Farajpour, A. and Mohammadi, M. (2016), "Vibration of piezoelectric nanofilm-based electromechanical sensors via higher-order non-local strain gradient theory", *IET Micro Nano Lett.*, **11**(6), 302-307. https://doi.org/10.1049/mnl.2016.0081

Farajpour, M.R., Shahidi, A. and Farajpour, A. (2018), "Resonant frequency tuning of nanobeams by piezoelectric nanowires under thermo-electro-magnetic field: A theoretical study", *Micro Nano Lett.*, **13**(11), 1627-1632. https://doi.org/10.1049/mnl.2018.5286

Fourn, H., Atmane, H.A., Bourada, M., Bousahla, A.A., Tounsi, A. and Mahmoud, S. (2018), "A novel four variable refined plate theory for wave propagation in functionally graded material plates", *Steel Compos. Struct.*, **27**(1), 109-122. http://doi.org/10.12989/scs.2018.27.1.109

Güven, U. (2014), "Transverse vibrations of single-walled carbon nanotubes with initial stress under magnetic field", *Compos. Struct.*, **114**, 92-98. https://doi.org/10.1016/j.compstruct.2014.03.054.

Hamza-Cherif, R., Meradjah, M., Zidour, M., Tounsi, A., Belmahi, S. and Bensattalah, T. (2018). "Vibration analysis of nano beam using differential transform method including thermal effect", *J. Nano Res.*, **54**(1-14), https://doi.org/10.4028/www.scientific.net/JNanoR.54.1.

Heireche, H., Tounsi, A., Benzair, A. and Mechab, I. (2008), "Sound wave propagation in single-walled carbon nanotubes with initial axial stress", *J. Appl. Physics*, **104**(1), 014301. https://doi.org/10.1063/1.2949274.

Kadari, B., Bessaim, A., Tounsi, A., Heireche, H., Bousahla, A.A. and Houari, M.S.A. (2018), "Buckling analysis of orthotropic nanoscale plates resting on elastic foundations", *J. Nano Res.*, **55**, 42-56. https://doi.org/10.4028/www.scientific.net/JNanoR.55.42.

Kahn, H., Huff, M. and Heuer, A. (1998), "The TiNi shape-memory alloy and its applications for MEMS", *J. Micromech. Microeng.*, **8**(3), 213.

Karami, B., Janghorban, M. and Tounsi, A. (2017), "Effects of triaxial magnetic field on the anisotropic nanoplates", *Steel Compos. Struct.*, **25**(3), 361-374. https://doi.org/10.12989/scs.2017.25.3.361.

Karami, B., Janghorban, M. and Tounsi, A. (2018), "Nonlocal strain gradient 3D elasticity theory for anisotropic spherical nanoparticles", *Steel Compos. Struct.*, **27**(2), 201-216. https://doi.org/10.12989/scs.2018.27.2.201.

Karami, B., Janghorban, M. and Tounsi, A. (2018), "Variational approach for wave dispersion in anisotropic doubly-curved nanoshells based on a new nonlocal strain gradient higher order shell theory", *Thin-Walled Struct.*, **129**, 251-264. https://doi.org/10.1016/j.tws.2018.02.025.

Karami, B., Shahsavari, D., Janghorban, M. and Li, L. (2018), "Wave dispersion of mounted graphene with initial stress", *Thin-Walled Struct.*, **122**, 102-111. https://doi.org/10.1016/j.tws.2017.10.004.

Khetir, H., Bouiadjra, M.B., Houari, M.S.A., Tounsi, A. and Mahmoud, S. (2017), "A new nonlocal trigonometric shear deformation theory for thermal buckling analysis of embedded nanosize FG plates", *Struct. Eng. Mech.*, **64**(4), 391-402. https://doi.org/10.12989/sem.2017.64.4.391.

Kiani, K., Gharebaghi, S.A. and Mehri, B. (2017), "In-plane and out-of-plane waves in nanoplates immersed in bidirectional magnetic fields", *Struct. Eng. Mech.*, **61**(1), 65-76. https://doi.org/10.12989/sem.2017.61.1.065.

Ma, L., Ke, L., Reddy, J., Yang, J., Kitipornchai, S. and Wang, Y. (2018), "Wave propagation characteristics in magneto-electro-elastic nanoshells using nonlocal strain gradient theory", *Compos. Struct.*, **199**, 10-23. https://doi.org/10.1016/j.compstruct.2018.05.061.

Malekzadeh, P. and Shojaee, M. (2013), "Free vibration of nanoplates based on a nonlocal two-variable refined plate theory", *Compos. Struct.*, **95**, 443-452. https://doi.org/10.1016/j.compstruct.2012.07.006.

Mohammadi, M., Farajpour, A. and Goodarzi, M. (2014), "Numerical study of the effect of shear in-plane load on the vibration analysis of graphene sheet embedded in an elastic medium", *Comput. Mater. Sci.*, **82**, 510-520. https://doi.org/10.1016/j.commatsci.2013.10.022.

Mokhtar, Y., Heireche, H., Bousahla, A.A., Houari, M.S.A., Tounsi, A. and Mahmoud, S. (2018), "A novel shear deformation theory for buckling analysis of single layer graphene sheet based on nonlocal elasticity theory", *Smart Struct. Syst*, **21**(4), 397-405. http://doi.org/10.12989/sss.2018.21.4.397

Mouffoki, A., Bedia, E., Houari, M.S.A., Tounsi, A. and Mahmoud, S. (2017), "Vibration analysis of nonlocal advanced nanobeams in hygro-thermal environment using a new two-unknown trigonometric shear deformation beam theory", *Smart Struct. Syst*, **20**(3), 369-383. https://doi.org/10.12989/sss.2017.20.3.369.

Murmu, T. and Pradhan, S. (2009), "Vibration analysis of nanoplates under uniaxial prestressed conditions via nonlocal elasticity", *J. Appl. Phys.*, **106**(10), 104301. https://doi.org/10.1063/1.3233914.

Nejad, M.Z., Hadi, A. and Farajpour, A. (2017), "Consistent couple-stress theory for free vibration analysis of Euler-Bernoulli nano-beams made of arbitrary bi-directional functionally graded materials", *Struct. Eng. Mech.*, **63**(2), 161-169. https://doi.org/10.12989/sem.2017.63.2.161.

Park, J.-S., Kim, J.-H. and Moon, S.-H. (2004), "Vibration of thermally post-buckled composite plates embedded with shape memory alloy fibers", *Compos. Struct.*, **63**(2), 179-188. https://doi.org/10.1016/S0263-8223(03)00146-6.

Reddy, J. (2007), "Nonlocal theories for bending, buckling and vibration of beams", *Eng. Sci.*, **45**(2-8), 288-307. https://doi.org/10.1016/j.ijengsci.2007.04.004.

Reddy, J. (2010), "Nonlocal nonlinear formulations for bending of classical and shear deformation theories of beams and plates", *J. Eng. Sci.*, **48**(11), 1507-1518. https://doi.org/10.1016/j.ijengsci.2010.09.020.
Reddy, J. and Pang, S. (2008), "Nonlocal continuum theories of beams for the analysis of carbon nanotubes", *J. Appl. Phys.*, **103**(2), 023511. https://doi.org/10.1063/1.2833431.
Selim, M., Abe, S. and Harigaya, K. (2009), "Effects of initial compression stress on wave propagation in carbon nanotubes", *Europ. Phys. J. B*, **69**(4), 523-528. https://doi.org/10.1140/epjb/e2009-00184-5.
Shen, Z.B., Tang, G.J., Zhang, L. and Li, X.F. (2012), "Vibration of double-walled carbon nanotube based nanomechanical sensor with initial axial stress", *Comput. Mater. Sci.*, **58**, 51-58. https://doi.org/10.1016/j.commatsci.2012.02.011.
Shenas, A.G. and Malekzadeh, P. (2016), "Free vibration of functionally graded quadrilateral microplates in thermal environment", *Thin-Walled Struct.*, **106**, 294-315. https://doi.org/10.1016/j.tws.2016.05.001.
Song, J., Shen, J. and Li, X. (2010), "Effects of initial axial stress on waves propagating in carbon nanotubes using a generalized nonlocal model", *Comput. Mater. Sci.*, **49**(3), 518-523. https://doi.org/10.1016/j.commatsci.2010.05.043.
Wang, X. and Cai, H. (2006), "Effects of initial stress on non-coaxial resonance of multi-wall carbon nanotubes", *Acta Materialia*, **54**(8), 2067-2074. https://doi.org/10.1016/j.actamat.2005.12.039.
Wang, Y.-Z., Li, F.-M. and Kishimoto, K. (2010), "Flexural wave propagation in double-layered nanoplates with small scale effects", *J. Appl. Phys.*, **108**(6), 064519. https://doi.org/10.1063/1.3481438.
Wang, Y.-Z., Li, F.-M. and Kishimoto, K. (2010), "Scale effects on flexural wave propagation in nanoplate embedded in elastic matrix with initial stress", *Appl. Physics A*, **99**(4), 907-911. https://doi.org/10.1007/s00339-010-5666-4.
Yahia, S.A., Atmane, H.A., Houari, M.S.A. and Tounsi, A. (2015), "Wave propagation in functionally graded plates with porosities using various higher-order shear deformation plate theories", *Struct. Eng. Mech*, **53**(6), 1143-1165. http://doi.org/10.12989/sem.2015.53.6.1143.
Yazid, M., Heireche, H., Tounsi, A., Bousahla, A.A. and Houari, M.S.A. (2018), "A novel nonlocal refined plate theory for stability response of orthotropic single-layer graphene sheet resting on elastic medium", *Smart Struct. Syst*, **21**(1), 15-25. http://doi.org/10.12989/sss.2018.21.1.015
Youcef, D.O., Kaci, A., Benzair, A., Bousahla, A.A. and Tounsi, A. (2018), "Dynamic analysis of nanoscale beams including surface stress effects", *Smart Struct. Syst*, **21**(1), 65-74. http://doi.org/10.12989/sss.2018.21.1.065.
Zemri, A., Houari, M.S.A., Bousahla, A.A. and Tounsi, A. (2015), "A mechanical response of functionally graded nanoscale beam: an assessment of a refined nonlocal shear deformation theory beam theory", *Struct. Eng. Mech.*, **54**(4), 693-710. https://doi.org/10.12989/sem.2015.54.4.693.
Zenkour, A. (2018), "Nonlocal elasticity and shear deformation effects on thermal buckling of a CNT embedded in a viscoelastic medium", *European Phys. J. Plus*, **133**(5), 196. https://doi.org/10.1140/epjp/i2018-12014-2.
Zenkour, A. and Sobhy, M. (2013), "Nonlocal elasticity theory for thermal buckling of nanoplates lying on Winkler–Pasternak elastic substrate medium", *Physica E*, **53**, 251-259. https://doi.org/10.1016/j.physe.2013.04.022.
Zenkour, A.M. and Sobhy, M. (2015), "A simplified shear and normal deformations nonlocal theory for bending of nanobeams in thermal environment", *Physica E*, **70**, 121-128. https://doi.org/10.1016/j.physe.2015.02.022.

CC

Appendix A

For a particular type of nanofibers such as shape memory alloy nanofibers, Brinson's model can be used to obtain the elasticity modulus of nanofibers (Brinson 1993)

$$E_F(\zeta) = \frac{E_{aus}E_{mar}}{\zeta E_{aus} + (1-\zeta)E_{mar}}, \tag{A1}$$

where "*aus*" and "*mar*" represent the nanofiber austenite and martensite phases, respectively. ξ can be expressed as

$$\zeta = \zeta_{str} + \zeta_{tem}. \tag{A2}$$

where

$$\begin{aligned} \zeta_{str} &= \zeta_{str0} - \frac{(\zeta_0 - \zeta)}{\zeta_0}\zeta_{str0}, \\ \zeta_{tem} &= \zeta_{tem0} - \frac{(\zeta_0 - \zeta)}{\zeta_0}\zeta_{tem0}. \end{aligned} \tag{A3}$$

In the above equations, "0", "tem" and "str" stand for the initial condition, temperature and stress, respectively. Applying Brinson's model, the following equation is also introduced for ξ

$$\begin{aligned} &\zeta = \frac{\zeta_0}{2}\left(1+\cos\left[\gamma_A\left(C_A T - \sigma - C_A A_{sta}\right)\right]\right) \\ &\text{for } T>A_{sta} \text{ and } C_A\left(T - A_{fin}\right) < \sigma < C_A\left(T - A_{sta}\right), \end{aligned} \tag{A4}$$

where

$$\gamma_A = \pi\left[C_A\left(A_{fin} - A_{sta}\right)\right]^{-1}. \tag{A5}$$

Here σ and T are respectively the stress and temperature; C_A, A_{fin} and A_{sta}, respectively, indicate the critical stress slope, finish and start temperatures for the austenite phase.

Appendix B

To give more detail about the derivation of the governing differential equations, the motion equation along the x direction, as an example, is derived in the following. Other motion equations are derived in a similar way. Using Eqs. (5), (9), (10) and (12), the force resultants are obtained as

$$\begin{aligned} N_{xx} &= \tilde{K}_{11}e^0_{xx} + \tilde{K}_{12}e^0_{yy} + \tilde{K}_{16}\gamma^0_{xy} \\ &-\left(\tilde{F}_{11}\kappa_{xx} + \tilde{F}_{12}\kappa_{yy} + \tilde{F}_{16}\kappa_{xy}\right) + N^{RS}_{xx} + \eta_{nl}\nabla^2 N_{xx}, \\ N_{yy} &= \tilde{K}_{12}e^0_{xx} + \tilde{K}_{22}e^0_{yy} + \tilde{K}_{26}\gamma^0_{xy} \\ &-\left(\tilde{F}_{12}\kappa_{xx} + \tilde{F}_{22}\kappa_{yy} + \tilde{F}_{26}\kappa_{xy}\right) + N^{RS}_{yy} + \eta_{nl}\nabla^2 N_{yy}, \\ N_{xy} &= \tilde{K}_{16}e^0_{xx} + \tilde{K}_{26}e^0_{yy} + \tilde{K}_{66}\gamma^0_{xy} \\ &-\left(\tilde{F}_{16}\kappa_{xx} + \tilde{F}_{26}\kappa_{yy} + \tilde{F}_{66}\kappa_{xy}\right) + N^{RS}_{xy} + \eta_{nl}\nabla^2 N_{xy}. \end{aligned} \tag{B1}$$

Substituting the right-hand sides of Eq. (B1) into Eq. (14), one obtains

$$\begin{aligned} &\tilde{K}_{11}\frac{\partial^2 u}{\partial x^2} + \tilde{K}_{66}\frac{\partial^2 u}{\partial y^2} + 2\tilde{K}_{16}\frac{\partial^2 u}{\partial x \partial y} \\ &+\tilde{K}_{16}\frac{\partial^2 v}{\partial x^2} + \tilde{K}_{26}\frac{\partial^2 v}{\partial y^2} + \left(\tilde{K}_{12} + \tilde{K}_{66}\right)\frac{\partial^2 v}{\partial x \partial y} \\ &-\left(\tilde{F}_{11}\frac{\partial^3 w}{\partial x^3} + \left(\tilde{F}_{12} + 2\tilde{F}_{66}\right)\frac{\partial^3 w}{\partial x \partial y^2} + 3\tilde{F}_{16}\frac{\partial^3 w}{\partial y \partial x^2} + \tilde{F}_{26}\frac{\partial^3 w}{\partial y^3}\right) \\ &+\eta_{nl}\nabla^2\left(\frac{\partial N_{xx}}{\partial x} + \frac{\partial N_{xy}}{\partial y}\right) = m_{sys}\frac{\partial^2 u}{\partial t^2}. \end{aligned} \tag{B2}$$

Again using Eq. (14), the last term on the right-hand side of Eq. (B2) is obtained as

$$\eta_{nl}\nabla^2\left(\frac{\partial N_{xx}}{\partial x} + \frac{\partial N_{xy}}{\partial y}\right) = m_{sys}\eta_{nl}\nabla^2\frac{\partial^2 u}{\partial t^2}. \tag{B3}$$

Now substituting Eq. (B3) into Eq. (B2) gives the motion equation along the x direction

$$\begin{aligned} &\tilde{K}_{11}\frac{\partial^2 u}{\partial x^2} + \tilde{K}_{66}\frac{\partial^2 u}{\partial y^2} + 2\tilde{K}_{16}\frac{\partial^2 u}{\partial x \partial y} + \left(\tilde{K}_{66} + \tilde{K}_{12}\right)\frac{\partial^2 v}{\partial x \partial y} \\ &+\tilde{K}_{16}\frac{\partial^2 v}{\partial x^2} + \tilde{K}_{26}\frac{\partial^2 v}{\partial y^2} - \left(\tilde{F}_{11}\frac{\partial^3 w}{\partial x^3} + \left(\tilde{F}_{12} + 2\tilde{F}_{66}\right)\frac{\partial^3 w}{\partial x \partial y^2}\right. \\ &\left.+3\tilde{F}_{16}\frac{\partial^3 w}{\partial y \partial x^2} + \tilde{F}_{26}\frac{\partial^3 w}{\partial y^3}\right) = m_{sys}\frac{\partial^2 u}{\partial t^2} - m_{sys}\eta_{nl}\nabla^2\frac{\partial^2 u}{\partial t^2}. \end{aligned} \tag{B4}$$

It should be noticed that the differential equations of motions along the y and z directions are derived in a similar way.